Radiation Report

TLV1H103-SEP Single-Event Effects (SEE) Radiation Report

1 TLV1H103-SEP Single-Event Effects (SEE) Radiation Report

The purpose of this study was to characterize the effects of heavy-ion irradiation on the single-event latch-up (SEL) performance of the TLV1H103-SEP 5.5V, high speed comparator. Heavy-ions with an LET_{EFF} of 48.47MeV-cm^2/mg were used to irradiate the device with a fluence of 1 × 10^7 ions/cm^2. The results demonstrate that the TLV1H103-SEP is SEL-immune up to LET_{EFF} = 43MeV-cm^2/mg at 125°C.

Characterization of single-event transients (SET) was also performed, up to a surface LET_{EFF} = 50MeV-cm^2 / mg at 125°C.

Table of Contents

Trademarks

All trademarks are the property of their respective owners.

2 Overview

The TLV1H103-SEP is a 325MHz, high-speed comparator with rail-to-rail inputs and a propagation delay of 2.5ns. The combination of fast response and wide operating voltage range make the comparators suitable for narrow signal pulse detection and data and clock recovery applications in LIDAR, range finders, and line receivers.

www.ti.com/product/TLV1H103-SEP

Table 2-1. Overview Information

DESCRIPTION	DEVICE INFORMATION
TI Part Number	TLV1H103-SEP
MLS Number	TLV1H103MDBVTSEP
Device Function	Radiation Tolerant 325MHz High-Speed Comparator with 2.5ns Propagation Delay in Space Enhanced Plastic
Technology	50BICOM3ZL
Exposure Facility	Process Radiation Effects Facility, Cyclotron Institute, Texas A&M University
Heavy Ion Fluence per Run	1×10^7 ions/cm^2
Irradiation Temperature	125°C (for SEL testing)

3 SEE Mechanisms

The primary single-event effect (SEE) events of interest in the TLV1H103-SEP are single-event latch-up (SEL). From a risk/impact point-of-view, the occurrence of an SEL is potentially the most destructive SEE event and the biggest concern for space applications. The 50BICOM3ZL process was used for the TLV1H103-SEP. CMOS circuitry introduces a potential for SEL susceptibility. SEL can occur if excess current injection caused by the passage of an energetic ion is high enough to trigger the formation of a parasitic cross-coupled PNP and NPN bipolar structure (formed between the p-sub and n-well and n+ and p+ contacts). The parasitic bipolar structure initiated by a single-event creates a high-conductance path (inducing a steady-state current that is typically orders-of-magnitude higher than the normal operating current) between power and ground that persists (is “latched”) until power is removed or until the device is destroyed by the high-current state. The process modifications applied for SEL-mitigation were sufficient as the TLV1H103-SEP exhibited no SEL with heavy-ions up to an LET_{EFF} of 43 MeV-cm^2/mg at a fluence of 10^7 ions/cm^2 and a chip temperature of 125°C.

This study was performed to evaluate the SEL effects with a bias voltage of 5.5V on Vcc Supply Voltage. Heavy ions with LET_{EFF} =48.47 MeV-cm^2/mg were used to irradiate the devices. Flux of 10^5 ions/s-cm^2 and fluence of 10^7 ions/cm^2 were used during the exposure at 125°C temperature.

4 Test Device and Test Board Information

The TLV1H103-SEP is packaged in a 6-pin, SOT-23 shown with pinout in Figure 4-1.

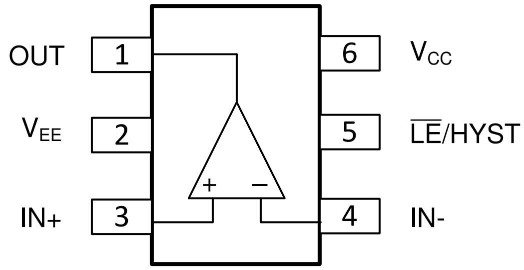

Figure 4-1. TLV1H103-SEP Pinout Diagram

Qualification Devices and Test Board

The TLV1H103-SEP was biased in either an output high or output low condition in single supply, where V_{CC} was set to 5.5V and V_{EE} was set to GND (0V). To achieve an output high state, IN+ was biased with 2V and IN- was biased with 1V. For an output low condition, IN+ was biased with 1V and IN- was biased with 2V. In either cases, the $\overline{LE}$/HYST pin was left open. Heavy ions with LETEFF = 48.47 MeV-cm^2 / mg were used to irradiate the devices. A nominal flux of 10^5 ions / s-cm^2 and fluence of 10^7 ions / cm^2 were used during the exposure at 125°C.

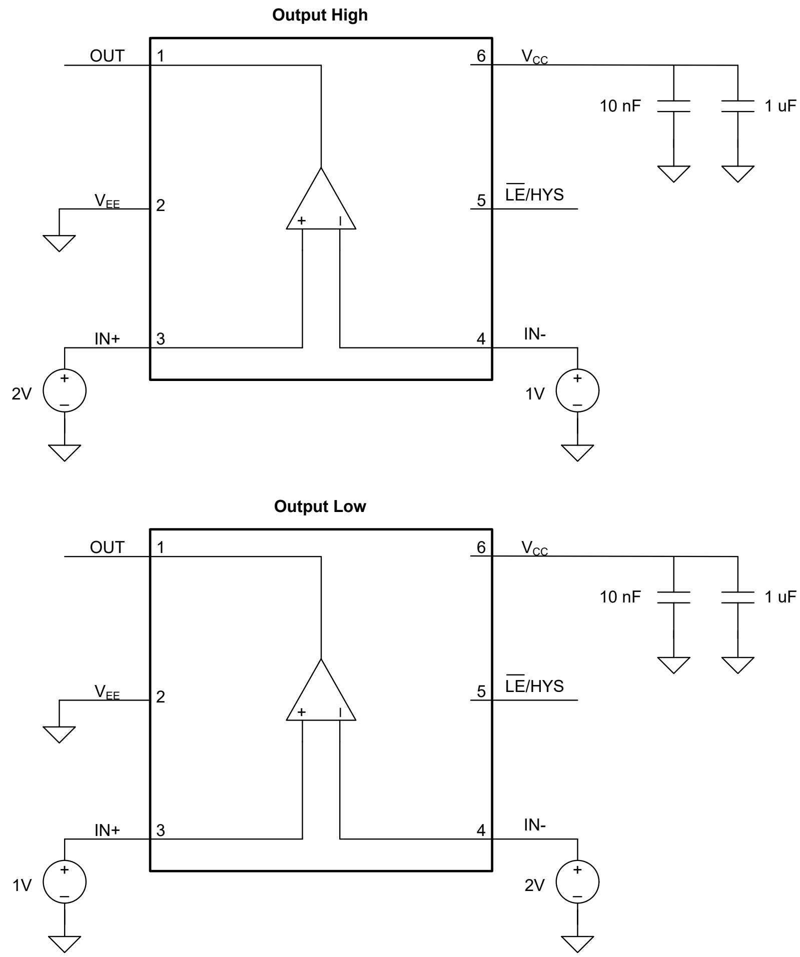

Figure 4-2. TLV1H103-SEP Bias Diagram

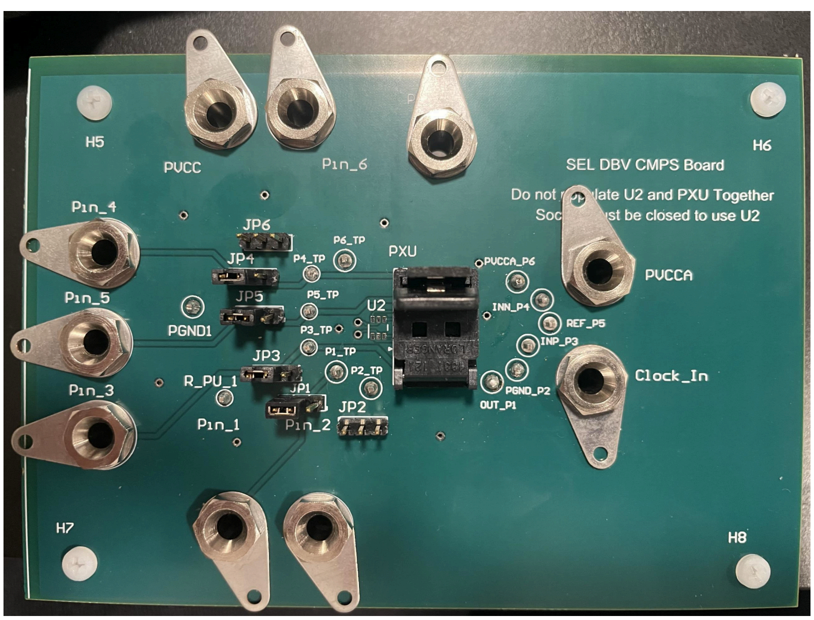

Figure 4-3. TLV1H103-SEP Bias Board for SEL Testing

5 Irradiation Facility and Setup

The heavy ion species used for the SEE studies on this product were provided and delivered by the TAMU Cyclotron Radiation Effects Facility using a superconducting cyclotron and advanced electron cyclotron resonance (ECR) ion source. Ion beams are delivered with high uniformity over a 1 inch diameter circular cross sectional area for the in-air station. Uniformity is achieved by means of magnetic defocusing. The intensity of the beam is regulated over a broad range spanning several orders of magnitude. For the bulk of these studies, ion fluxes between 10^4 and 10^5ions / s-cm^2 were used to provide heavy ion fluences of 10^7ions/cm^2. For these experiments Silver (Ag) ions were used. Ion beam uniformity for all tests was 95%.

6 Results

6.1 Single Event Latchup (SEL) Results

During SEL characterization, the device was heated using forced hot air, maintaining the IC temperature at 125°C. The temperature was monitored by means of a K-type thermocouple attached as close as possible to the IC. The species used for the SEL testing was a silver (^{47}Ag) ion with an angle-of-incidence of 0° for an LET_{EFF} = 48.47MeV-cm^2/mg. The kinetic energy in the vacuum for this ion is 1.634GeV (15MeV/amu line). A flux of approximately 10^{5}ions/cm^2-s and a fluence of approximately 10^7 ions were used. The supply voltage is supplied externally on board at recommended maximum voltage setting of 5.5V. Run duration to achieve this fluence was approximately less than 2 minutes. Two devices were tested where one device was biased in an output high condition and the other device was biased in an output low condition. Each device had three runs.

Table 6-1. TLV1H103-SEP SEL Conditions Using^{47}Ag at an Angle-of-Incidence of 0°

RUN #	DUT	Output Condition	DISTANCE (mm)	TEMPERATURE (°C)	ION	ANGLE	FLUX (ions·cm^2/mg)	FLUENCE (# ions)	LET_{EFF} (MeV.cm^2/mg)
8	2	Low	40	125	Ag	0	1.17E+05	1.00 E+07	48.47
9	2	Low	40	125	Ag	0	1.18E+05	1.00 E+07	48.47
10	2	Low	40	125	Ag	0	1.2E+05	1.00 E+07	48.47
11	3	High	40	125	Ag	0	1.22E+05	1.00 E+07	48.47
12	3	High	40	125	Ag	0	1.18E+05	1.00 E+07	48.47
13	3	High	40	125	Ag	0	1.23E+05	1.00 E+07	48.47

No SEL events were observed, indicating that the TLV1H103-SEP is SEL-immune at LET_{EFF} = 43MeV-cm^2/mg and T = 125°C. Using the MFTF method described in Section 9 and combining (or summing) the fluences of the three runs @ 125°C (3 × 10^7), the upper-bound cross-section (using a 95% confidence level) is calculated as:

$\sigma SEL \leq 1.23 \times 10^{-7}$ cm^2 for LET_{EFF} = 43MeV-cm^2/mg and T = 125°C.

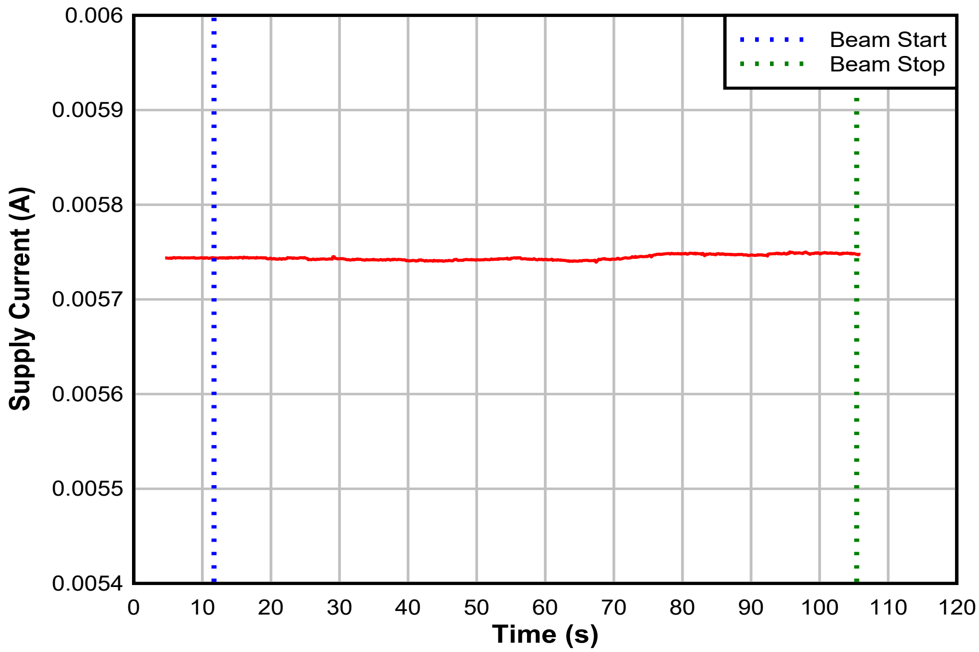

Figure 6-1. Run #8: DUT2 Supply Current vs. Time

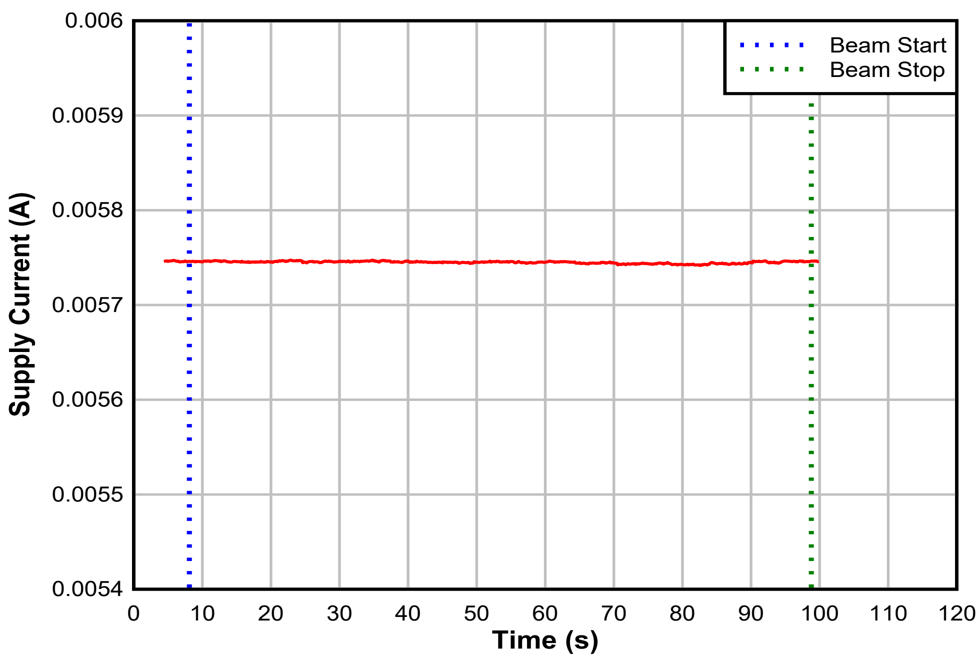

Figure 6-2. Run #9: DUT2 Supply Current vs. Time

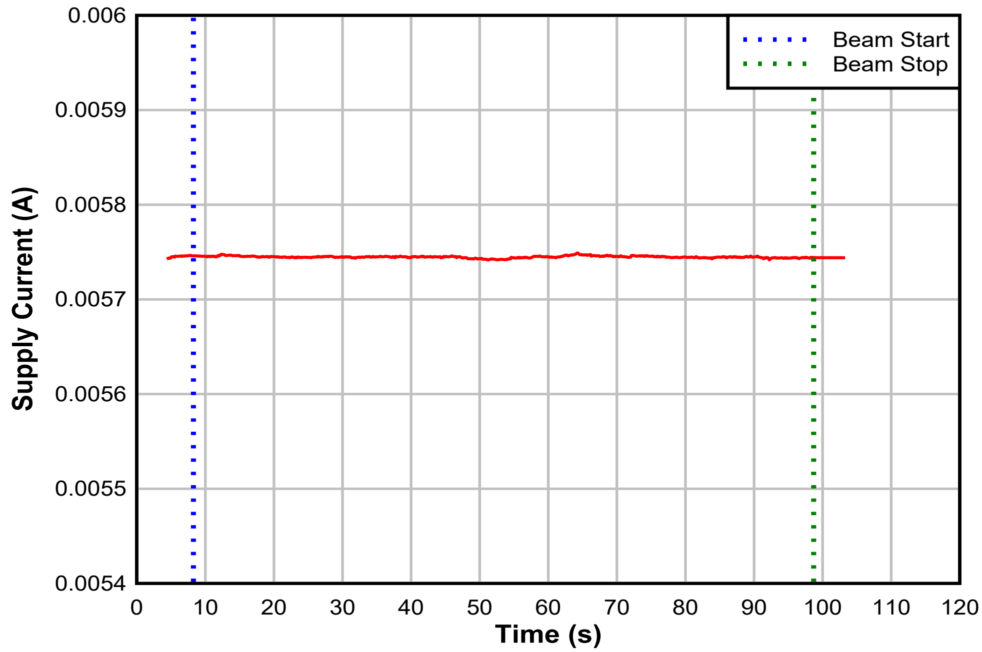

Figure 6-3. Run #10: DUT2 Supply Current vs. Time

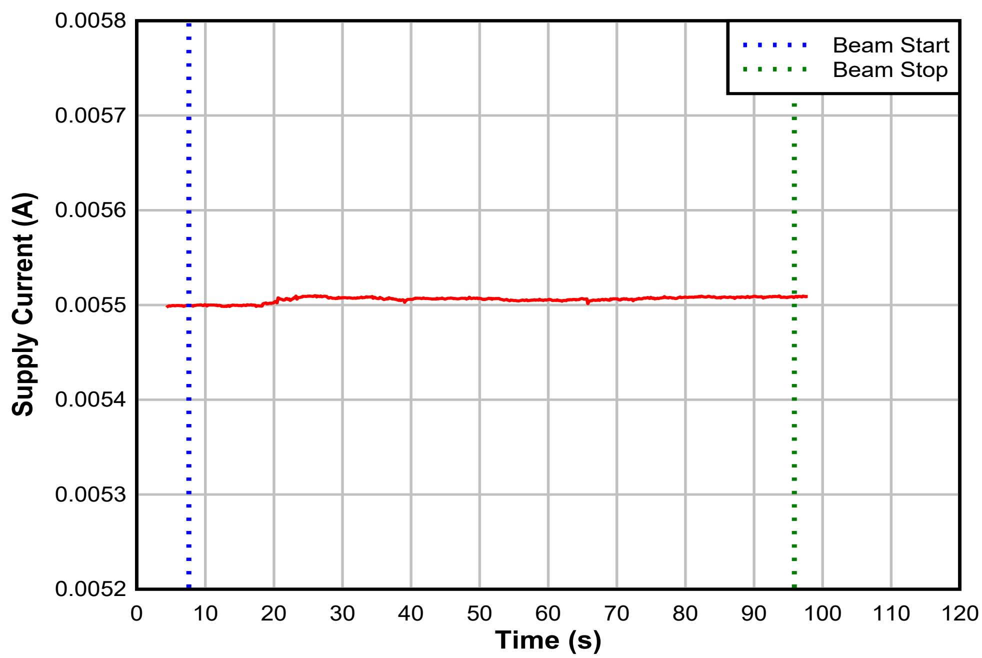

Figure 6-4. Run #11: DUT3 Supply Current vs. Time

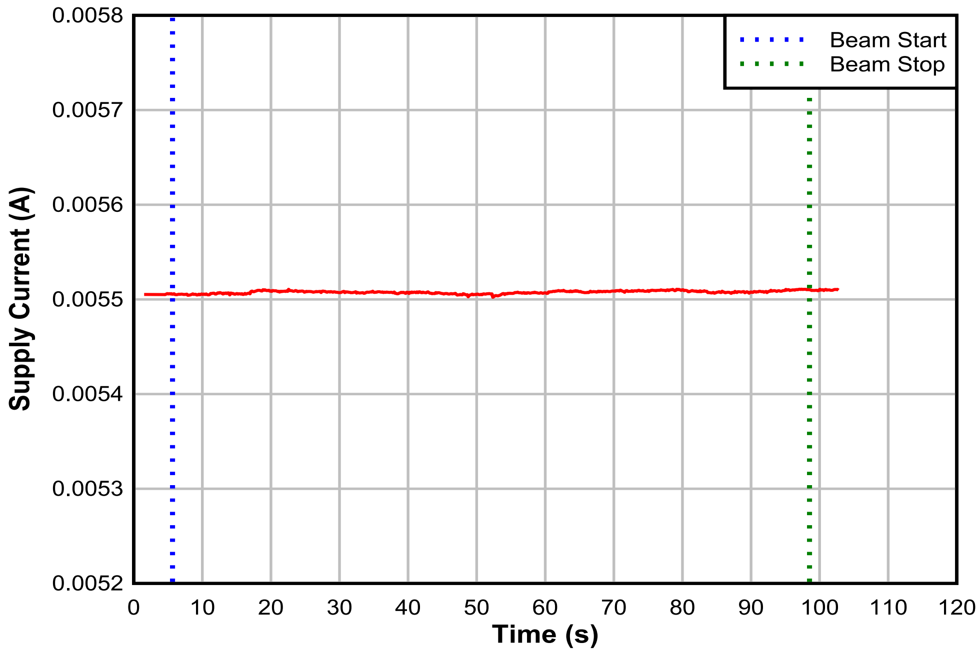

Figure 6-5. Run #12: DUT3 Supply Current vs. Time

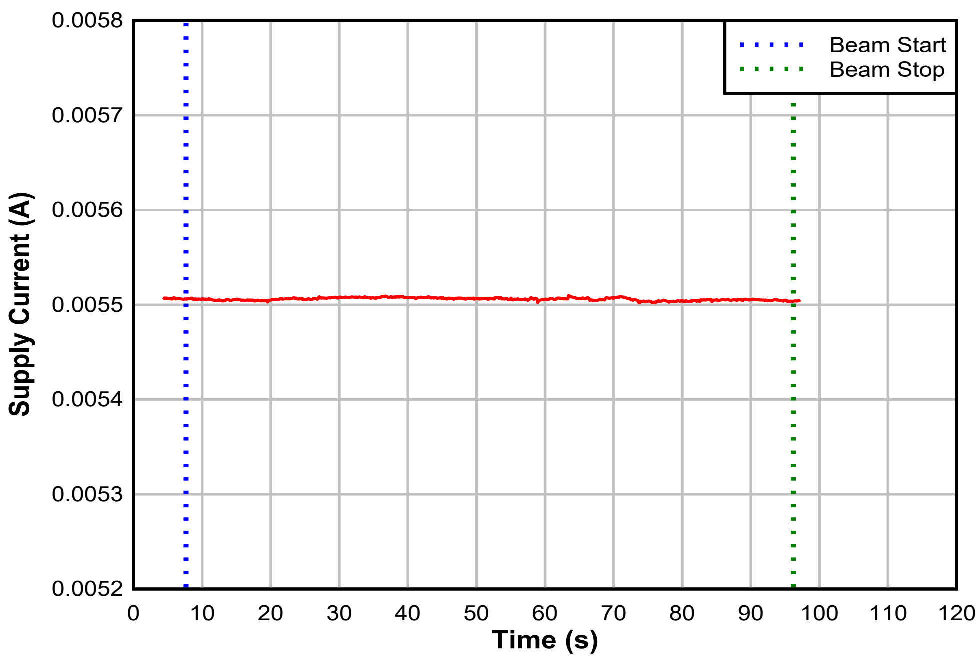

Figure 6-6. Run #13: DUT3 Supply Current vs. Time

6.2 Single Event Transient (SET) Results

The TLV1H103-SEP was characterized from 50.5 to 1.0 MeV-cm^2 / mg at 2.4V, 3.3V, and 5.5V supply voltages in both output high and output low configuration. The device was tested at room temperature for all SETs runs. A nominal flux of 10^5 ions / s-cm^2 was used, with each run concluding once a fluence of 10^7 ions/cm^2 was reached. The device was tested at approximately 25°C as it was exposed to six LET_{EFF} readpoints of 50.5 MeV-cm^2 / mg, 35.6 MeV-cm^2 / mg, 23.1 MeV-cm^2 / mg, 9.8 MeV-cm^2 / mg, 5.3 MeV-cm^2 / mg, and 1.0 MeV-cm^2 / mg. The output was monitored with the oscilloscope set to a window trigger mode that captured any events where the output shifted by ±250mV or more. The conditions and results for each run are summarized in the tables below. See SET Results Appendix for histograms of the transient magnitudes and transient waveforms.

Table 6-2. SET Run Summary for TLV1H103-SEP in Output High Condition

RUN #	DUT	Output Condition	TEMPERATURE (°C)	ION	ANGLE	FLUX (ions·cm²/mg)	FLUENCE (# ions)	LET_{EFF} (MeV.cm²/mg)	$V_s = V_{CC} - V_{EE}$	# of Events
32	4	High	25	Xe	0	1.020 E+05	1.00 E+07	50.5	2.4	178
33	4	High	25	Xe	0	1.023 E+05	1.00 E+07	50.5	3.3	174
34	4	High	25	Xe	0	1.010 E+05	1.00 E+07	50.5	5.5	329
113	4	High	25	Kr	0	1.122 E+05	1.00 E+07	35.6	2.4	81
114	4	High	25	Kr	0	1.129 E+05	1.00 E+07	35.6	3.3	132
116	4	High	25	Kr	0	1.066 E+05	1.00 E+07	35.6	5.5	238
173	4	High	25	Kr	0	0.989 E+05	1.00 E+07	23.1	2.4	39
174	4	High	25	Kr	0	1.025 E+05	1.00 E+07	23.1	3.3	66
176	4	High	25	Kr	0	1.041 E+05	1.00 E+07	23.1	5.5	95
192	4	High	25	Ar	0	0.998 E+05	1.00 E+07	9.8	2.4	13
193	4	High	25	Ar	0	0.999 E+05	1.00 E+07	9.8	3.3	18
194	4	High	25	Ar	0	0.982 E+05	1.00 E+07	9.8	5.5	59
202	4	High	25	Ar	0	0.924 E+05	1.00 E+07	5.3	2.4	0
203	4	High	25	Ar	0	0.945 E+05	1.00 E+07	5.3	3.3	1
204	4	High	25	Ar	0	0.956 E+05	1.00 E+07	5.3	5.5	2
288	4	High	25	O	0	1.059 E+05	1.00 E+07	1.0	2.4	0
289	4	High	25	O	0	1.069 E+05	1.00 E+07	1.0	3.3	0
290	4	High	25	O	0	1.081 E+05	1.00 E+07	1.0	5.5	0

Table 6-3. SET Run Summary for TLV1H103-SEP in Output Low Condition

RUN #	DUT	Output Condition	TEMPERATURE (°C)	ION	ANGLE	FLUX (ions·cm²/mg)	FLUENCE (# ions)	LET_{EFF} (MeV.cm²/mg)	$V_s = V_{CC} - V_{EE}$	# of Events
35	4	Low	25	Xe	0	1.019 E+05	1.00 E+07	50.5	2.4	93
36	4	Low	25	Xe	0	1.025 E+05	1.00 E+07	50.5	3.3	102
37	4	Low	25	Xe	0	1.019 E+05	1.00 E+07	50.5	5.5	303

Table 6-3. SET Run Summary for TLV1H103-SEP in Output Low Condition (continued)

RUN #	DUT	Output Condition	TEMPERATURE (°C)	ION	ANGLE	FLUX (ions·cm²/mg)	FLUENCE (# ions)	LET_{EFF} (MeV.cm²/mg)	$V_s = V_{CC} - V_{EE}$	# of Events
117	4	Low	25	Kr	0	1.045 E+05	1.00 E+07	35.6	2.4	61
118	4	Low	25	Kr	0	1.039 E+05	1.00 E+07	35.6	3.3	69
119	4	Low	25	Kr	0	1.051 E+05	1.00 E+07	35.6	5.5	170
177	4	Low	25	Kr	0	1.039 E+05	1.00 E+07	23.1	2.4	34
178	4	Low	25	Kr	0	1.011 E+05	1.00 E+07	23.1	3.3	48
179	4	Low	25	Kr	0	0.992 E+05	1.00 E+07	23.1	5.5	70
195	4	Low	25	Ar	0	0.978 E+05	1.00 E+07	9.8	2.4	0
196	4	Low	25	Ar	0	0.981 E+05	1.00 E+07	9.8	3.3	2
197	4	Low	25	Ar	0	0.980 E+05	1.00 E+07	9.8	5.5	2
198	4	Low	25	Ar	0	0.973 E+05	1.00 E+07	5.3	2.4	0
199	4	Low	25	Ar	0	0.945 E+05	1.00 E+07	5.3	3.3	0
200	4	Low	25	Ar	0	0.934 E+05	1.00 E+07	5.3	5.5	0
291	4	Low	25	O	0	1.079 E+05	1.00 E+07	1.0	2.4	0
292	4	Low	25	O	0	1.065 E+05	1.00 E+07	1.0	3.3	0
293	4	Low	25	O	0	1.069 E+05	1.00 E+07	1.0	5.5	0

Figures 6-7 to 6-10 show two examples of a typical transient event at 5.5V supply and LET_{EFF} = 50.5 MeV-cm^2 / mg. Their corresponding supply current was also recorded.

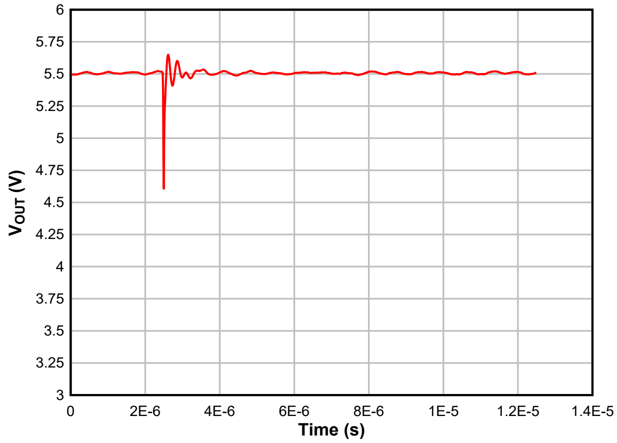

Figure 6-7. Run 34, Event 90, Output High

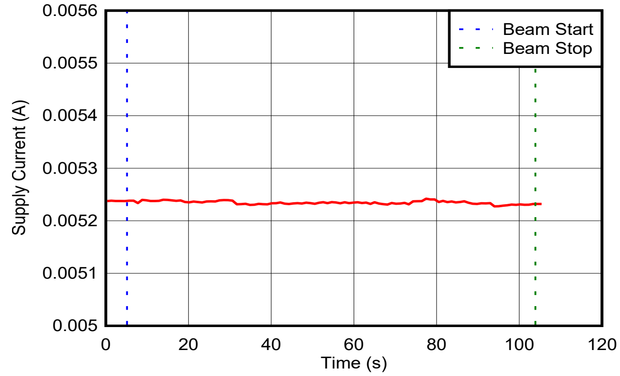

Figure 6-8. Run 34, Event 90, Supply Current

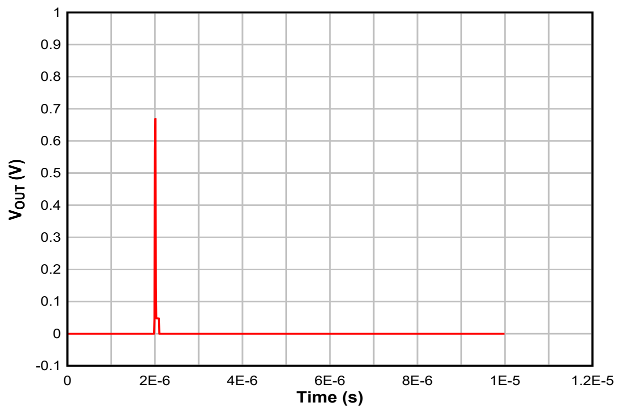

Figure 6-9. Run 37, Event 148, Output Low

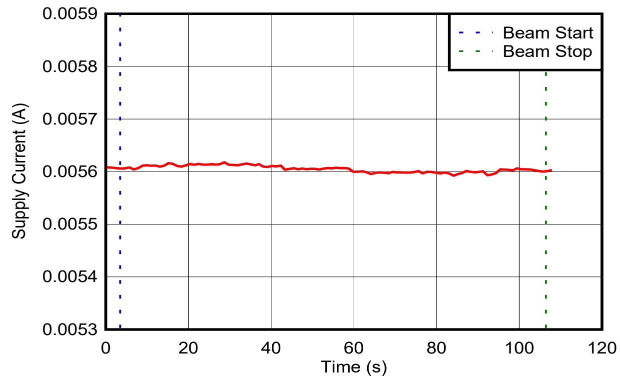

Figure 6-10. Run 37, Event 148, Supply Current

Weibull Fit

Weibull-Fit and cross section plots for the TLV1H103-SEP at supply voltages of 2.4V, 3.3V, and 5.5V are shown in the figures below respectively. For each of the supply voltages, the total number of transients (both output high and output low combined) and the run fluences are used to calculate the mean (σ_{MEAN}), upper bound (σ_{UB}), and lower bound (σ_{LB}) cross section (as discussed in Appendix C) at 95% confidence interval. The Weibull equation used for the fit is presented in Equation 1, and parameters are shown in Table 6-10.

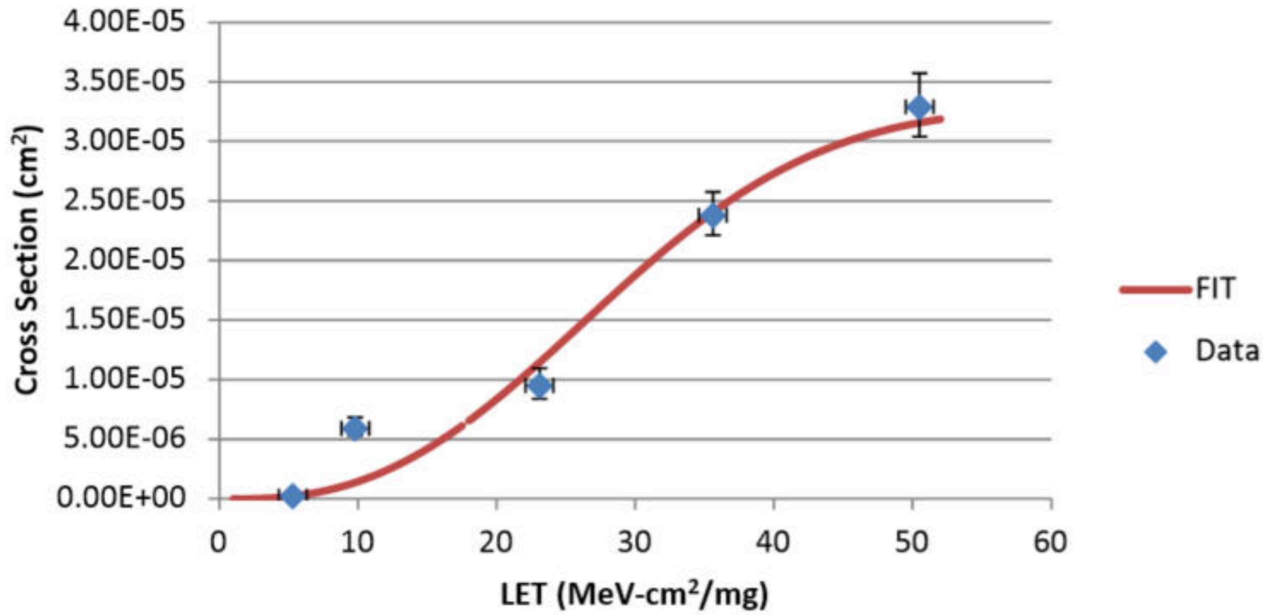

Figure 6-11. Cross Section and Weibull Fit for 2.4V Supply, Output Low

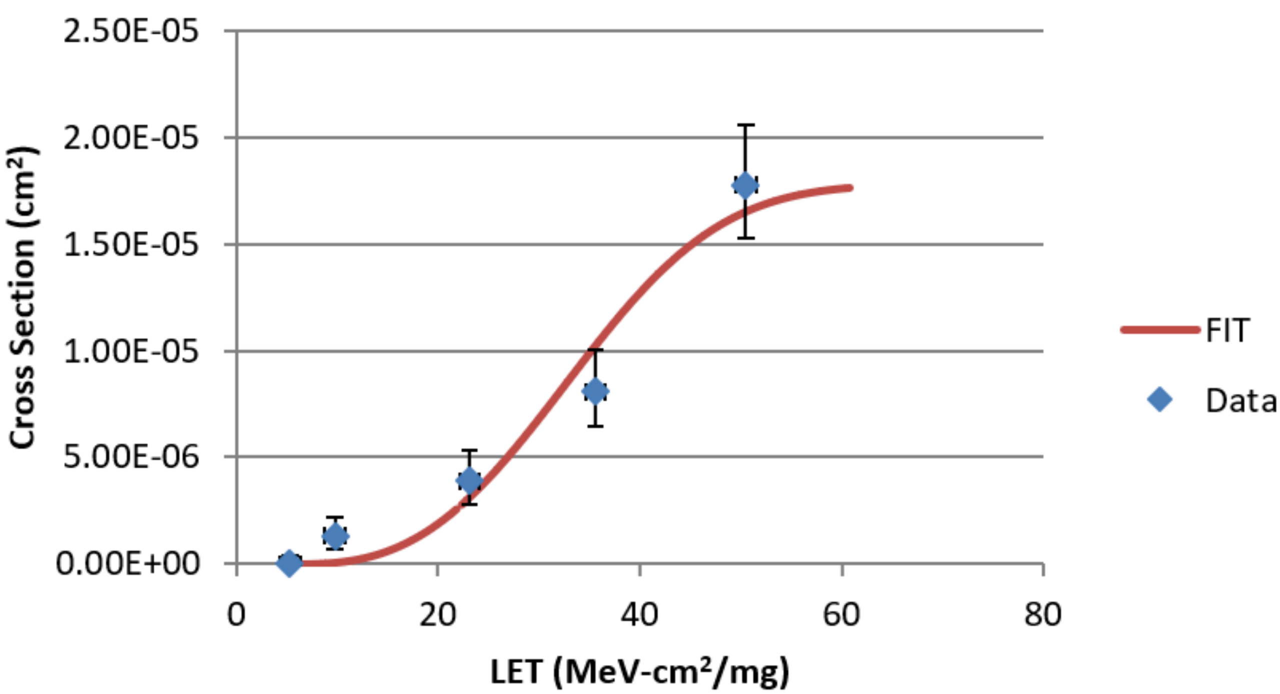

Figure 6-12. Cross Section and Weibull Fit for 2.4V Supply, Output High

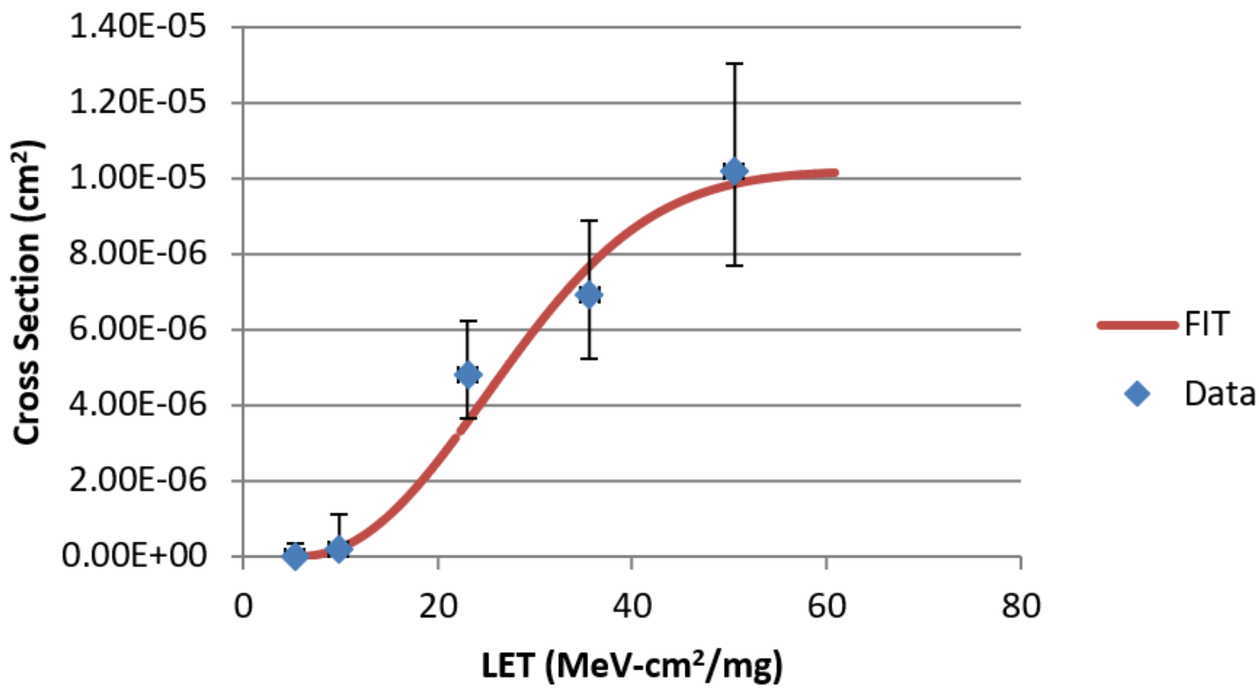

Figure 6-13. Cross Section and Weibull Fit for 3.3V Supply, Output Low

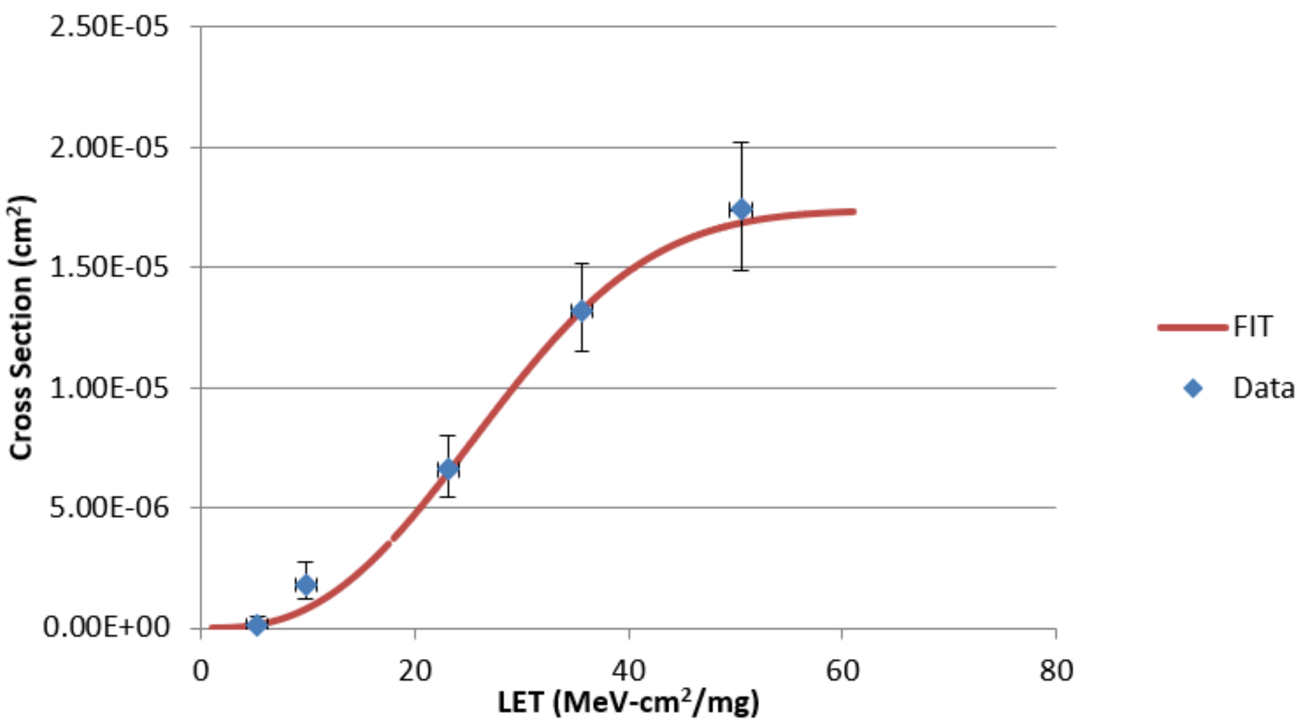

Figure 6-14. Cross Section and Weibull Fit for 3.3V Supply, Output High

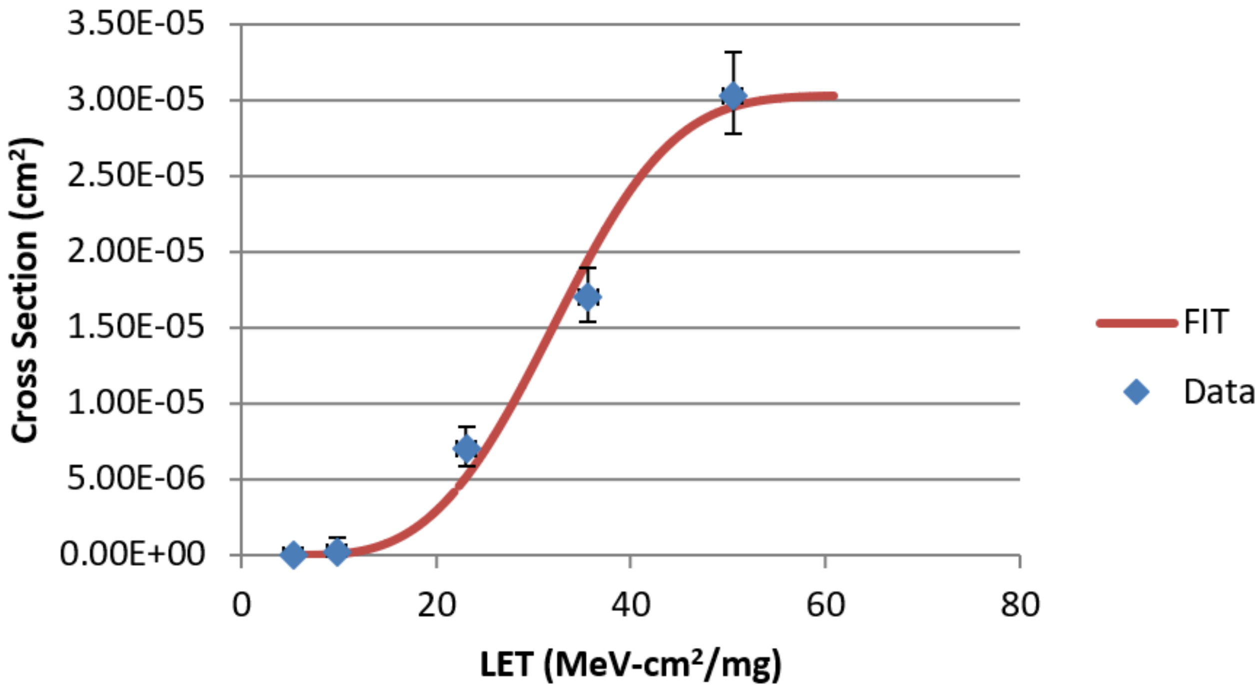

Figure 6-15. Cross Section and Weibull Fit for 5.5V Supply, Output Low

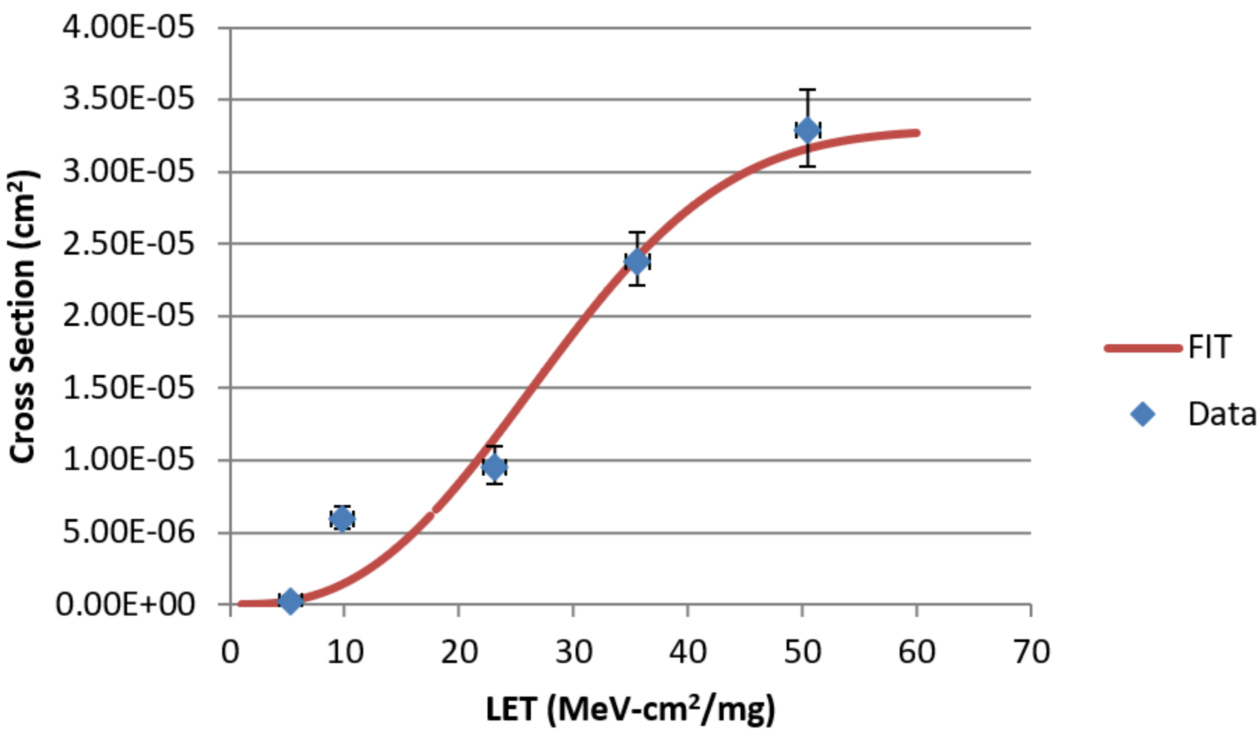

Figure 6-16. Cross Section and Weibull Fit for 5.5V Supply, Output High

Table 6-4. Cross Section and Weibull Fit Data: 2.4V Supply, Output Low

LET_{EFF}(MeV-cm^2 /mg)	Ion	Fluence (Ions/cm^2)	Total Events	σ_{LB} (cm^2/Device)	σ_{MEAN} (cm^2/Device)	FIT	Residual	Residual^2	σ_{UB} (cm^2/Device)	UB Error	LB Error
50.5	Xe	1.00E+07	93	7.51E-06	9.3E-06	8.85E-06	4.49E-07	2.01E-13	1.14E-05	2.09E-06	1.79E-06
35.6	Kr	1.00E+07	61	4.67E-06	6.1E-06	6.4E-06	-2.96E-07	8.78E-14	7.84E-06	1.74E-06	1.43E-06
23.1	Kr	1.00E+07	34	2.35E-06	3.4E-06	2.34E-06	1.06E-06	1.13E-12	4.75E-06	1.35E-06	1.05E-06
9.8	Ar	1.00E+07	0	0	0	0	0	0	3.69E-07	3.69E-07	0
5.3	Ar	1.00E+07	0	0	0	0	0	0	3.69E-07	3.69E-07	0
1.0	O	1.00E+07	0	0	0	0	0	0	3.69E-07	3.69E-07	0

Table 6-5. Cross Section and Weibull Fit Data: 2.4V Supply, Output High

Energy (MeV-cm^2 /mg)	Ion	Fluence (Ions/cm^2)	Total Events	σ_{LB} (cm^2/Device)	σ_{MEAN} (cm^2/Device)	FIT	Residual	Residual^2	σ_{UB} (cm^2/Device)	UB Error	LB Error
50.5	Xe	1.00E+07	178	1.53E-05	1.78E-05	1.65E-05	1.28E-06	1.65E-12	2.06E-05	2.82E-06	2.52E-06
35.6	Kr	1.00E+07	81	6.43E-06	8.1E-06	1.03E-05	-2.15E-06	4.64E-12	1.01E-05	1.97E-06	1.67E-06
23.1	Kr	1.00E+07	39	2.77E-06	3.9E-06	3.13E-06	7.68E-07	5.90E-13	5.33E-06	1.43E-06	1.13E-06
9.8	Ar	1.00E+07	13	1.07E-06	1.80E-06	7.31E-08	1.73E-06	2.98E-12	2.84E-06	1.04E-06	7.33E-07
5.3	Ar	1.00E+07	0	0	0	0	0	0	3.69E-07	3.69E-07	0
1.0	O	1.00E+07	0	0	0	0	0	0	3.69E-07	3.69E-07	0

Table 6-6. Cross Section and Weibull Fit Data: 3.3V Supply, Output Low

Energy (MeV-cm^2 /mg)	Ion	Fluence (Ions/cm^2)	Total Events	σ_{LB} (cm^2/Device)	σ_{MEAN} (cm^2/Device)	FIT	Residual	Residual^2	σ_{UB} (cm^2/Device)	UB Error	LB Error
50.5	Xe	1.00E+07	102	8.32E-06	1.02E-05	9.85E-06	3.49E-07	1.22E-13	1.24E-05	2.18E-6	1.88E-06
35.6	Kr	1.00E+07	69	5.37E-06	6.9E-06	7.69E-06	-7.86E-07	6.17E-13	8.73E-06	1.83E-06	1.53E-06
23.1	Kr	1.00E+07	48	3.54E-06	4.80E-06	3.59E-06	1.21E-06	1.45E-12	6.36E-06	1.56E-06	1.26E-06
9.8	Ar	1.00E+07	2	2.42E-08	2.00E-07	2.13E-07	-1.29E-08	1.66E-16	7.22E-07	5.22E-07	1.76E-07
5.3	Ar	1.00E+07	0	0	0	0	0	0	3.69E-07	3.69E-07	0
1.0	O	1.00E+07	0	0	0	0	0	0	3.69E-07	3.69E-07	0

Table 6-7. Cross Section and Weibull Fit Data: 3.3V Supply, Output High

Energy (MeV-cm^2 /mg)	Ion	Fluence (Ions/cm^2)	Total Events	σ_{LB} (cm^2/Device)	σ_{MEAN} (cm^2/Device)	FIT	Residual	Residual^2	σ_{UB} (cm^2/Device)	UB Error	LB Error
50.5	Xe	1.00E+07	174	1.49E-05	1.74E-05	1.69E-05	5.27E-07	2.78E-13	2.02E-05	2.79E-06	2.49E-06
35.6	Kr	1.00E+07	132	1.10E-05	1.32E-05	1.32E-05	-2.99E-08	8.92E-16	1.57E-05	2.45E-06	2.16E-06
23.1	Kr	1.00E+07	66	5.1E-06	6.60E-06	6.48E-06	1.21E-07	1.47E-14	8.40E-06	1.80E-06	1.50E-06
9.8	Ar	1.00E+07	18	1.07E-06	1.80E-06	7.92E-07	1.01E-06	1.02E-12	2.84E-06	1.04E-06	7.33E-07
5.3	Ar	1.00E+07	1	2.53E-09	1.00E-07	1.35E-07	-3.48E-08	1.21E-15	5.57E-07	4.57E-07	9.75E-08
1.0	O	1.00E+07	0	0	0	0	0	0	3.69E-07	3.69E-07	0

Table 6-8. Cross Section and Weibull Fit Data: 5.5V Supply, Output Low

Energy (MeV-cm^2 /mg)	Ion	Fluence (Ions/ cm^2)	Total Events	σ_{LB} (cm^2/ Device)	σ_{MEAN} (cm^2/ Device)	FIT	Residual	Residual^2	σ_{UB} (cm^2/ Device)	UB Error	LB Error
50.5	Xe	1.00E+07	303	2.70E-05	3.03E_05	2.96E-05	7.40E-07	5.47E-13	3.39E-05	3.61E-06	3.32E-06
35.6	Kr	1.00E+07	170	1.45E-05	1.70E-05	1.95E-05	-2.51E-06	6.29E-12	1.98E-05	2.76E-06	2.46E-06
23.1	Kr	1.00E+07	70	5.46E-06	7.00E-06	5.2E-06	1.80E-06	3.25E-12	8.84E-06	1.84E-06	1.54E-06
9.8	Ar	1.00E+07	2	2.42E-08	2.00E-07	6.99E-08	1.30E-07	1.69E-14	7.22E-07	5.22E-07	1.76E-07
5.3	Ar	1.00E+07	0	0	0	0	0	0	3.69E-07	3.69E-07	0
1.0	O	1.00E+07	0	0	0	0	0	0	3.69E-07	3.69E-07	0

Table 6-9. Cross Section and Weibull Fit Data: 5.5V Supply, Output High

Energy (MeV-cm^2 /mg)	Ion	Fluence (Ions/ cm^2)	Total Events	σ_{LB} (cm^2/ Device)	σ_{MEAN} (cm^2/ Device)	FIT	Residual	Residual^2	σ_{UB} (cm^2/ Device)	UB Error	LB Error
50.5	Xe	1.00E+07	329	2.94E-05	3.29E-05	3.16E-05	1.31E-06	1.72E-12	3.67E-05	3.75E-06	3.46E-06
35.6	Kr	1.00E+07	238	2.09E-05	2.38E-05	2.41E-05	-2.77E-07	7.66E-14	2.70E-05	3.22E-06	2.93E-06
23.1	Kr	1.00E+07	95	7.69E-06	9.50E-06	1.15E-05	-1.98E-06	3.92E-12	1.16E-05	2.11E-06	1.81E-06
9.8	Ar	1.00E+07	59	4.49E-06	5.90E-06	1.38E-06	4.52E-06	2.04E-11	7.61E-06	1.71E-06	1.41E-06
5.3	Ar	1.00E+07	2	2.42E-08	2.00E-07	2.35E-07	-3.49E-08	1.22E-15	7.22E-07	5.22E-07	1.76E-07
1.0	O	1.00E+07	0	0	0	0	0	0	3.69E-07	3.69E-07	0

$$\sigma = \sigma_{SAT} \cdot \left(1 - e^{\left(-\frac{LET - Onset}{W}\right)^{s}}\right) \tag{1}$$

Table 6-10. Weibull Fit Parameters

Parameters	Value for 2.4V Supply, Output Low	Value for 2.4V Supply, Output High	Value for 3.3V Supply, Output Low	Value for 3.3 V Supply, Output High	Value for 5.5V Supply, Output Low	Value for 5.5V Supply, Output High
σ_{SAT} (cm^2)	9.30E-06	1.78E-05	1.02E-05	1.74E-05	3.03E-05	3.29E-05
Onset (MeV-cm^2 /mg)	9.8	5.3	5.3	1	5.3	1
w	24	32	26	30	30	31
s	2.1	2.8	2.2	2.5	3.2	2.5
Sum (Residual^2)	1.42E-12	8.38E-12	2.19E-12	1.31E-12	1.01E-11	2.61E-11

7 Summary

Radiation effects of the radiation tolerant high speed comparator in space enhanced plastic TLV1H103-SEP was studied. This device passed total dose rate of up to 30krad(Si) and is SEL immune up to LET_{EFF} = 43MeV-cm^2/mg and T = 125°C. SET characterization of the device was also conducted.

8 SET Results Appendix

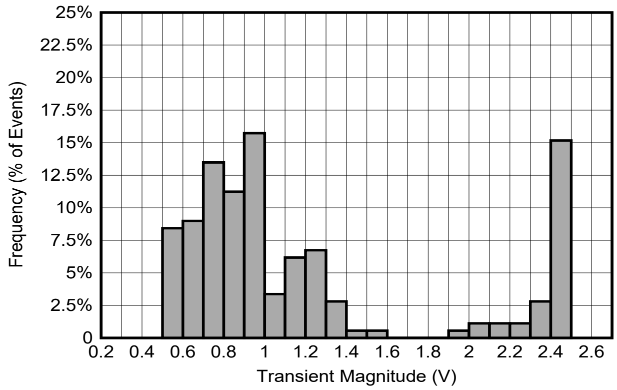

Figure 8-1. Transient Event Magnitude Histogram, 2.4V Supply, LET_{EFF} = 50.5MeV-cm^2 / mg, Output High Condition

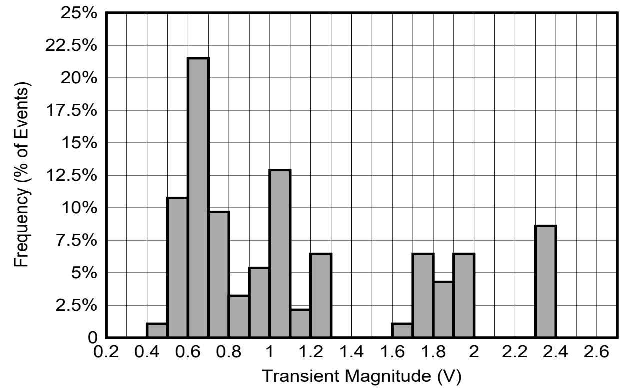

Figure 8-2. Transient Event Magnitude Histogram, 2.4V Supply, LET_{EFF} = 50.5MeV-cm^2 / mg, Output Low Condition

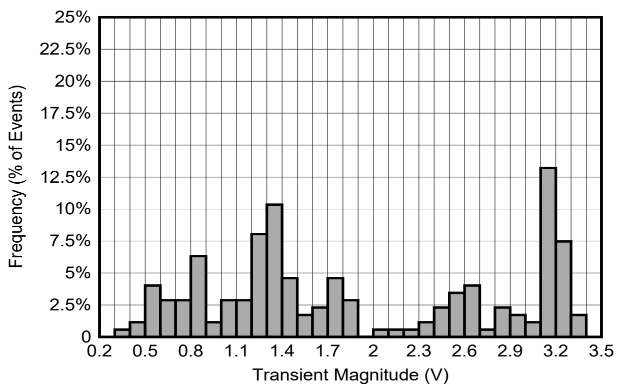

Figure 8-3. Transient Event Magnitude Histogram, 3.3V Supply, LET_{EFF} = 50.5MeV-cm^2 / mg, Output High Condition

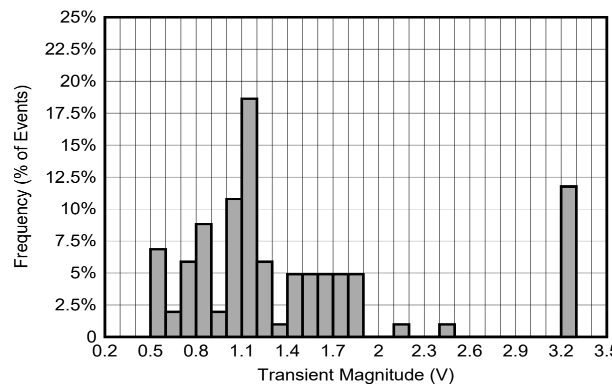

Figure 8-4. Transient Event Magnitude Histogram, 3.3V Supply, LET_{EFF} = 50.5MeV-cm^2 / mg, Output Low Condition

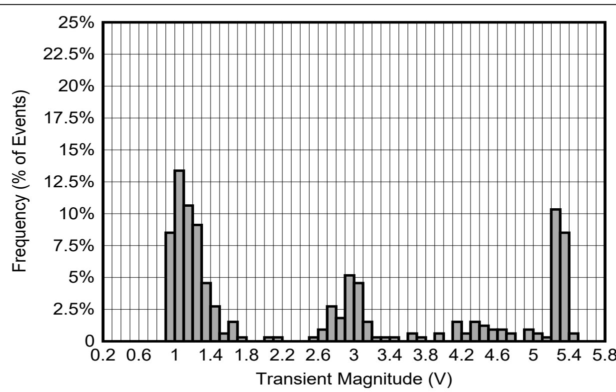

Figure 8-5. Transient Event Magnitude Histogram, 5.5V Supply, LET_{EFF} = 50.5MeV-cm^2 / mg, Output High Condition

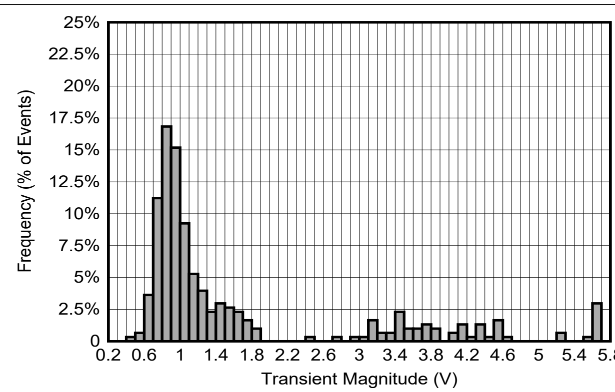

Figure 8-6. Transient Event Magnitude Histogram, 5.5V Supply, LET_{EFF} = 50.5MeV-cm^2 / mg, Output Low Condition

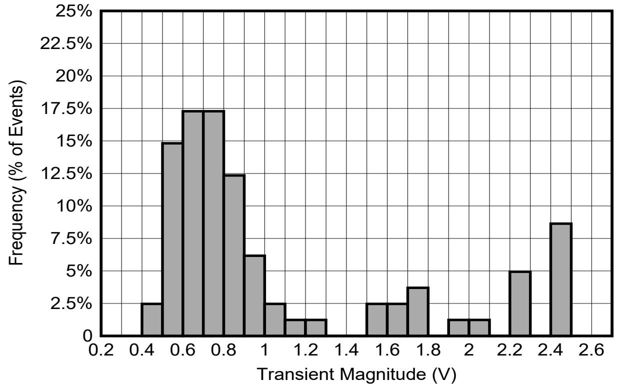

Figure 8-7. Transient Event Magnitude Histogram, 2.4V Supply, LET_{EFF} = 35.6MeV-cm^2 / mg, Output High Condition

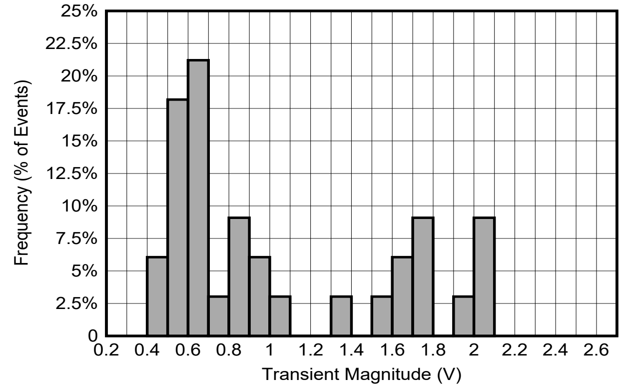

Figure 8-8. Transient Event Magnitude Histogram, 2.4V Supply, LET_{EFF} = 35.6MeV-cm^2 / mg, Output Low Condition

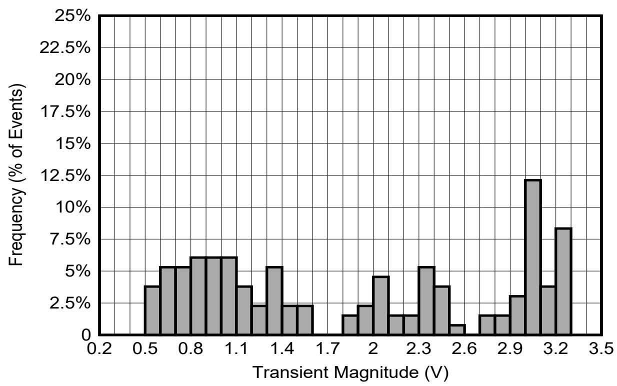

Figure 8-9. Transient Event Magnitude Histogram, 3.3V Supply, LET_{EFF} = 35.6MeV-cm^2 / mg, Output High Condition

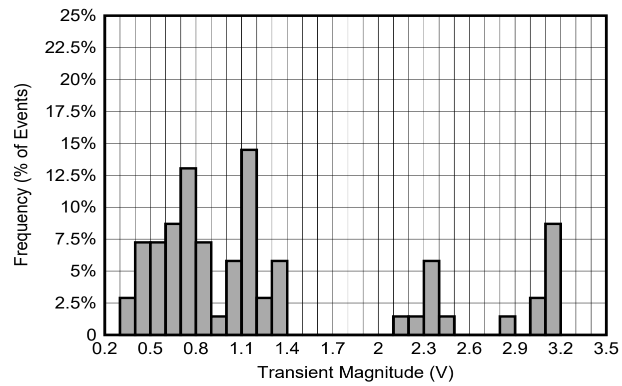

Figure 8-10. Transient Event Magnitude Histogram, 3.3V Supply, LET_{EFF} = 35.6MeV-cm^2 / mg, Output Low Condition

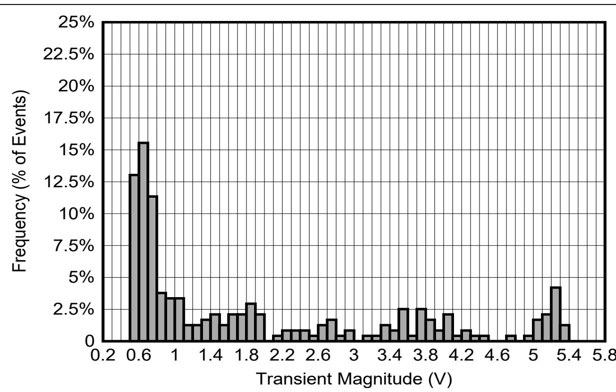

Figure 8-11. Transient Event Magnitude Histogram, 5.5V Supply, LET_{EFF} = 35.6MeV-cm^2 / mg, Output High Condition

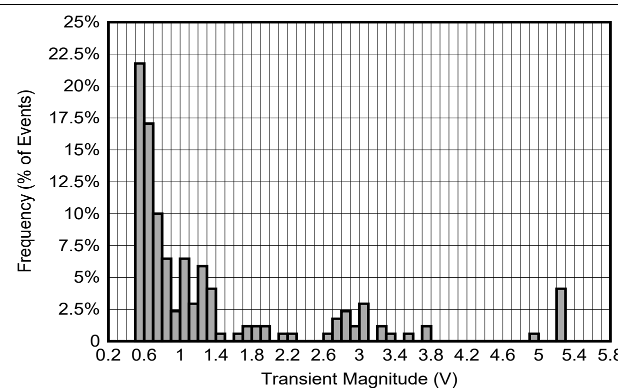

Figure 8-12. Transient Event Magnitude Histogram, 5.5V Supply, LET_{EFF} = 35.6MeV-cm^2 / mg, Output Low Condition

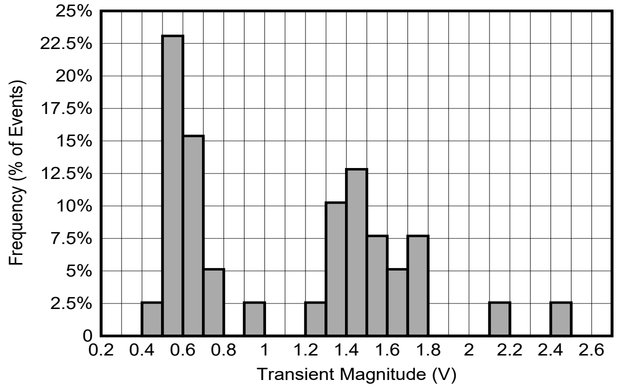

Figure 8-13. Transient Event Magnitude Histogram, 2.4V Supply, LET_{EFF} = 23.1MeV-cm^2 / mg, Output High Condition

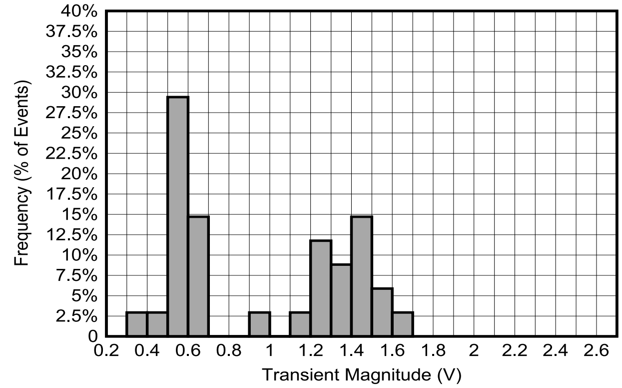

Figure 8-14. Transient Event Magnitude Histogram, 2.4V Supply, LET_{EFF} = 23.1MeV-cm^2 / mg, Output Low Condition

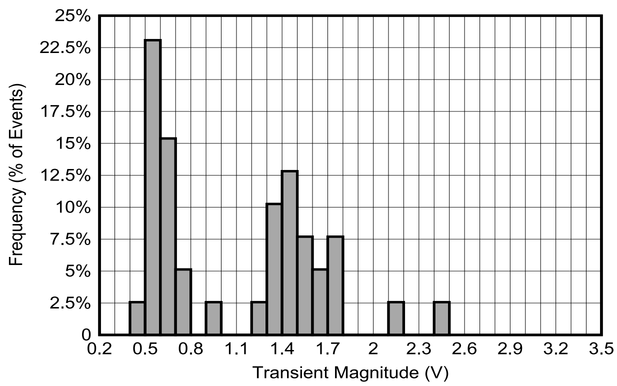

Figure 8-15. Transient Event Magnitude Histogram, 3.3V Supply, LET_{EFF} = 23.1MeV-cm^2 / mg, Output High Condition

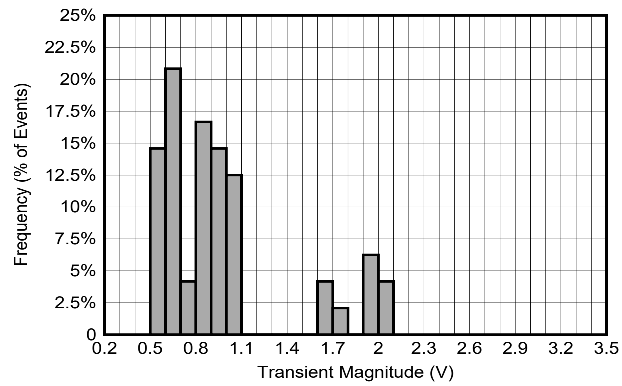

Figure 8-16. Transient Event Magnitude Histogram, 3.3V Supply, LET_{EFF} = 23.1MeV-cm^2 / mg, Output Low Condition

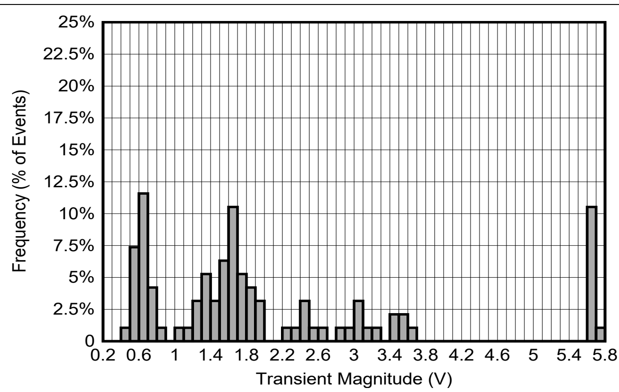

Figure 8-17. Transient Event Magnitude Histogram, 5.5V Supply, LET_{EFF} = 23.1MeV-cm^2 / mg, Output High Condition

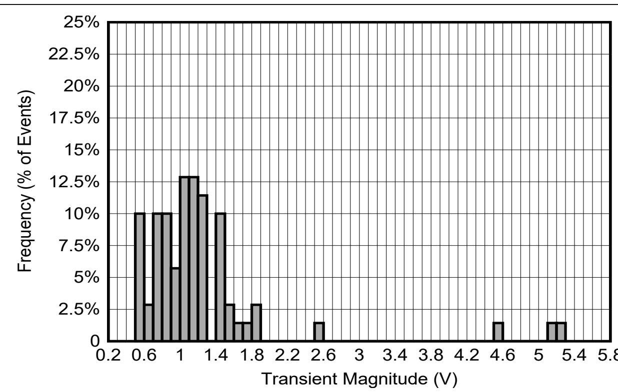

Figure 8-18. Transient Event Magnitude Histogram, 5.5V Supply, LET_{EFF} = 23.1MeV-cm^2 / mg, Output Low Condition

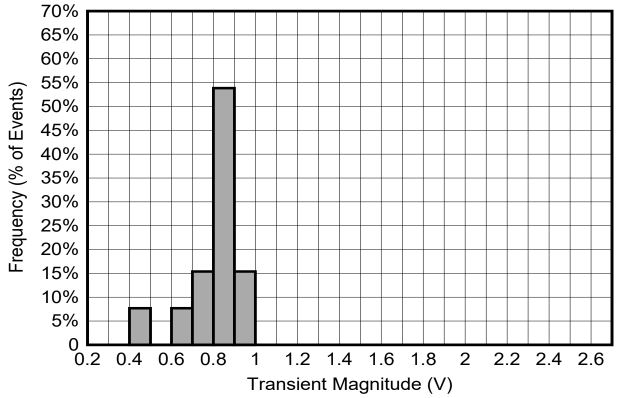

Figure 8-19. Transient Event Magnitude Histogram, 2.4V Supply, LET_{EFF} = 9.8MeV-cm^2 / mg, Output High Condition

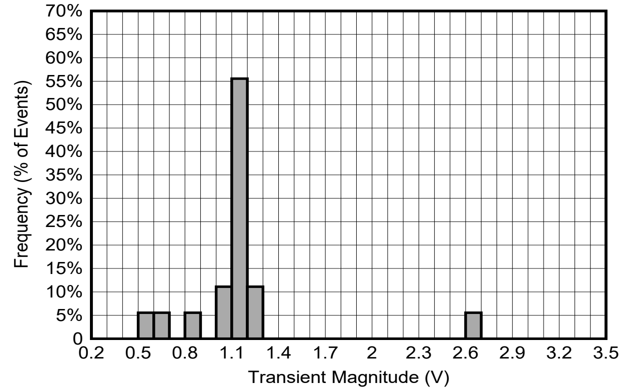

Figure 8-20. Transient Event Magnitude Histogram, 3.3V Supply, LET_{EFF} = 9.8MeV-cm^2 / mg, Output High Condition

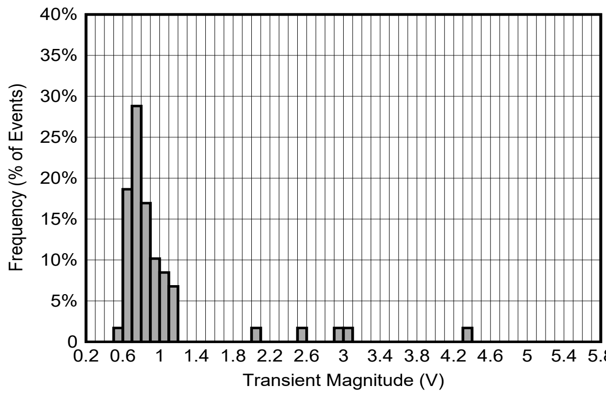

Figure 8-21. Transient Event Magnitude Histogram, 5.5V Supply, LET_{EFF} = 9.8MeV-cm^2 / mg, Output High Condition

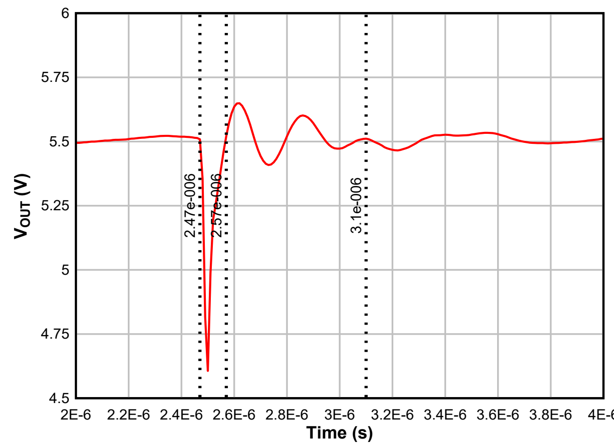

Figure 8-22. Run 34, Event 90, Zoomed in

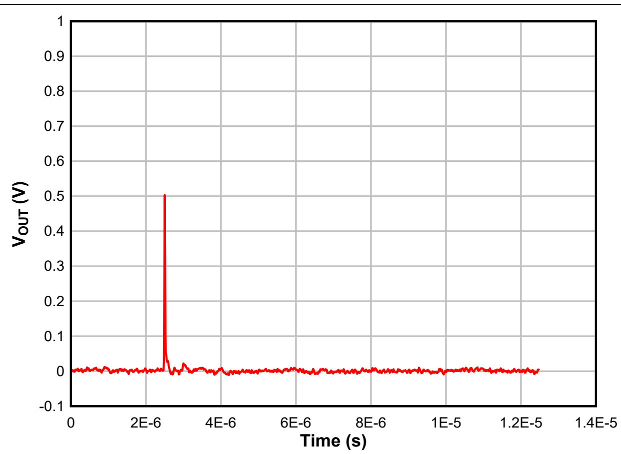

Figure 8-23. Run 196, Event 1, 3.3V Supply, LET_{EFF} = 9.8MeV-cm^2 / mg, Output Low Condition

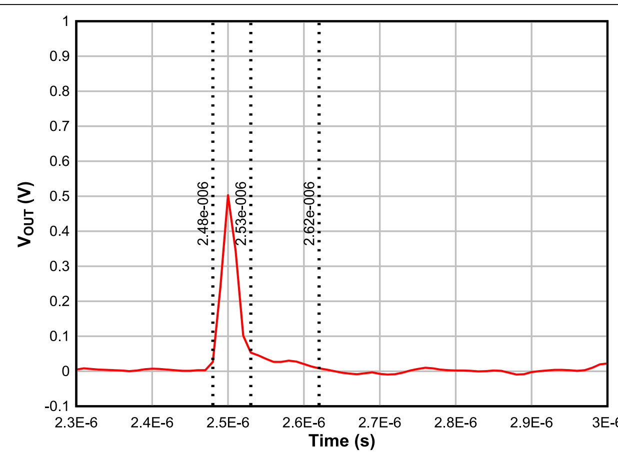

Figure 8-24. Run 196, Event 1, Zoomed In

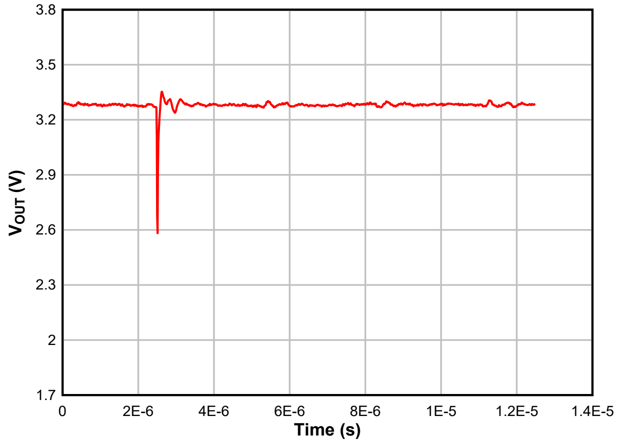

Figure 8-25. Run 203, Event 1, 3.3V Supply, LET_{EFF} = 5.3MeV-cm^2 / mg, Output High Condition

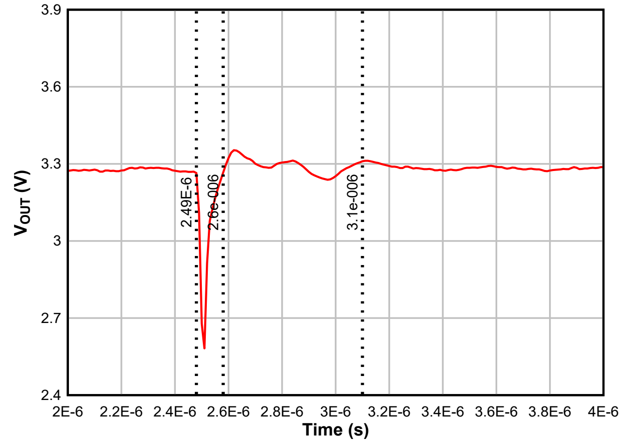

Figure 8-26. Run 203, Event 1, Zoomed In

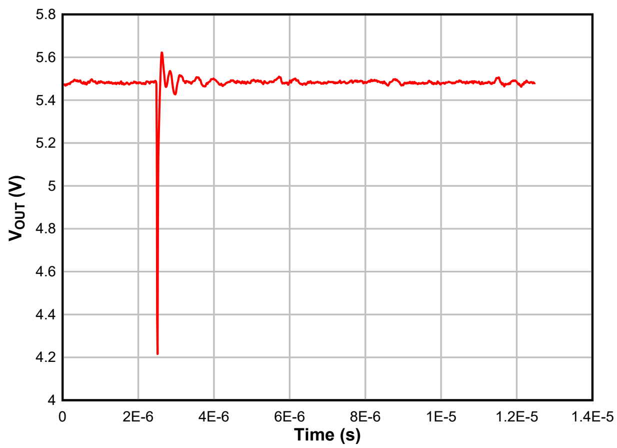

Figure 8-27. Run 204, Event 2, 5.5V Supply, LET_{EFF} = 5.3MeV-cm^2 / mg, Output High Condition

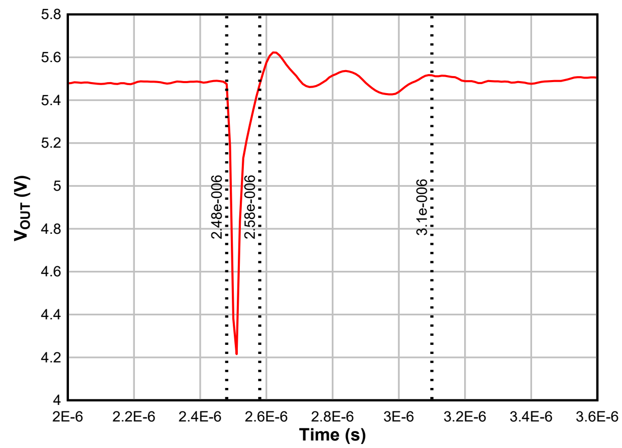

Figure 8-28. Run 204, Event 2, Zoomed In

9 Confidence Interval Calculations

For conventional products where hundreds of failures are seen during a single exposure, one can determine the average failure rate of parts being tested in a heavy-ion beam as a function of fluence with high degree of certainty and reasonably tight standard deviation, and thus have a good deal of confidence that the calculated cross-section is accurate.

With radiation hardened parts however, determining the cross-section becomes more difficult since often few, or even, no failures are observed during an entire exposure. Determining the cross-section using an average failure rate with standard deviation is no longer a viable option, and the common practice of assuming a single error occurred at the conclusion of a null-result can end up in a greatly underestimated cross-section.

In cases where observed failures are rare or non-existent, the use of confidence intervals and the chi-squared distribution is indicated. The Chi-Squared distribution is particularly well-suited for the determination of a reliability level when the failures occur at a constant rate. In the case of SEE testing, where the ion events are random in time and position within the irradiation area, one expects a failure rate that is independent of time (presuming that parametric shifts induced by the total ionizing dose do not affect the failure rate), and thus the use of chi-squared statistical techniques is valid (since events are rare an exponential or Poisson distribution is usually used).

In a typical SEE experiment, the device-under-test (DUT) is exposed to a known, fixed fluence (ions/cm^2) while the DUT is monitored for failures. This is analogous to fixed-time reliability testing and, more specifically, time-terminated testing, where the reliability test is terminated after a fixed amount of time whether or not a failure has occurred (in the case of SEE tests fluence is substituted for time and hence it is a fixed fluence testEquation 2). Calculating a confidence interval specifically provides a range of values which is likely to contain the parameter of interest (the actual number of failures/fluence). Confidence intervals are constructed at a specific confidence level. For example, a 95% confidence level implies that if a given number of units were sampled numerous times and a confidence interval estimated for each test, the resulting set of confidence intervals would bracket the true population parameter in about 95% of the cases.

In order to estimate the cross-section from a null-result (no fails observed for a given fluence) with a confidence interval, we start with the standard reliability determination of lower-bound (minimum) mean-time-to-failure for fixed-time testing (an exponential distribution is assumed):

$$MTTF = \frac{2nT}{\chi^2_{2(d+1);100\left(1-\frac{\alpha}{2}\right)}} \tag{2}$$

Where *MTTF* is the minimum (lower-bound) mean-time-to-failure, *n* is the number of units tested (presuming each unit is tested under identical conditions) and *T*, is the test time, and χ^2 is the chi-square distribution evaluated at 100(1 – α / 2) confidence level and where *d* is the degrees-of-freedom (the number of failures observed). With slight modification for our purposes we invert the inequality and substitute *F* (fluence) in the place of *T*:

$$MFTF = \frac{2nF}{\chi^2_{2(d+1);100\left(1-\frac{\alpha}{2}\right)}} \tag{3}$$

Where now *MFTF* is mean-fluence-to-failure and *F* is the test fluence, and as before, χ^2 is the chi-square distribution evaluated at 100(1 – α / 2) confidence and where *d* is the degrees-of-freedom (the number of failures observed). The inverse relation between *MTTF* and failure rate is mirrored with the *MFTF*. Thus the upper-bound cross-section is obtained by inverting the *MFTF*:

$$\sigma = \frac{\chi^2_{2(d+1);100\left(1-\frac{\alpha}{2}\right)}}{2nF} \tag{4}$$

Assume that all tests are terminated at a total fluence of 10^6 ions/cm^2. Also assume there are a number of devices with very different performances that are tested under identical conditions. Assume a 95% confidence level (σ = 0.05). Note that as *d* increases from 0 events to 100 events the actual confidence interval becomes smaller, indicating that the range of values of the true value of the population parameter (in this case the cross-section) is approaching the mean value + 1 standard deviation. This makes sense when one considers that as more events are observed the statistics are improved such that uncertainty in the actual device performance is reduced.

Table 9-1. Experimental Example Calculation of MFTF and σ Using a 95% Confidence Interval

Degrees-of-Freedom (d)	2(d + 1)	χ^2 @ 95%	Calculated Cross Section (cm^2)		
			Upper-Bound @ 95% Confidence	Mean	Average + Standard Deviation
0	2	7.38	3.69E–06	0.00E+00	0.00E+00
1	4	11.14	5.57E–06	1.00E–06	2.00E–06
2	6	14.45	7.22E–06	2.00E–06	3.41E–06
3	8	17.53	8.77E–06	3.00E–06	4.73E–06
4	10	20.48	1.02E–05	4.00E–06	6.00E–06
5	12	23.34	1.17E–05	5.00E–06	7.24E–06
10	22	36.78	1.84E–05	1.00E–05	1.32E–05
50	102	131.84	6.59E–05	5.00E–05	5.71E–05
100	202	243.25	1.22E–04	1.00E–04	1.10E–04

10 References

1. M. Shoga and D. Binder, "Theory of Single Event Latchup in Complementary Metal-Oxide Semiconductor Integrated Circuits", *IEEE Trans. Nucl. Sci., Vol. 33(6)*, Dec. 1986, pp. 1714-1717.
2. G. Bruguier and J. M. Palau, "Single particle-induced latchup", *IEEE Trans. Nucl. Sci., Vol. 43(2)*, Mar. 1996, pp. 522-532.
3. TAMU Radiation Effects Facility website. http://cyclotron.tamu.edu/ref/
4. "The Stopping and Range of Ions in Matter" (SRIM) software simulation tools website. www.srim.org/index.htm#SRIMMENU
5. D. Kececioglu, “Reliability and Life Testing Handbook”, Vol. 1, PTR Prentice Hall, New Jersey,1993, pp. 186-193.
6. ISDE CRÈME-MC website.https://creme.isde.vanderbilt.edu/CREME-MC
7. A. J. Tylka, J. H. Adams, P. R. Boberg, et al.,"CREME96: A Revision of the Cosmic Ray Effects on Micro-Electronics Code", *IEEE Trans. on Nucl. Sci., Vol. 44(6)*, Dec. 1997, pp. 2150-2160.
8. A. J. Tylka, W. F. Dietrich, and P. R. Boberg, "Probability distributions of high-energy solar-heavy-ion fluxes from IMP-8: 1973-1996", *IEEE Trans. on Nucl. Sci.,Vol. 44(6)*, Dec. 1997, pp. 2140-2149.

IMPORTANT NOTICE AND DISCLAIMER